Predicting Net Ecosystem Carbon Exchange of Typical Forest Ecosystems in China Based on ChinaFLUX

Jingjing Wu ¹, Qiaoli Wu ^{1*}, Wei He², Jie Jiang¹

- School of Geomatics and Urban Spatial Informatics, Beijing University of Civil Engineering and Architecture, Beijing 102616, China – jjwu0413@foxmail.com, wuqiaoli, jiangjie@bucea.edu.cn
 - 2. Zhejiang Carbon Neutral Innovation Institute, Zhejiang University of Technology, Hangzhou, Zhejiang 310014, China wei.he@zjut.edu.cn

Keywords: ChinaFLUX, Net Ecosystem Carbon Exchange, Forest Ecosystem, Long Short-Term Memory Network.

Abstract:

Accurate prediction of forest carbon sinks is crucial for achieving carbon neutrality, peak carbon emissions goals, and advancing the Sustainable Development Goals (SDGs). Due to the complexity of forest ecosystems and the limited application and accessibility of ChinaFLUX observation data, previous studies generating Net Ecosystem Exchange (NEE) products largely relied on global flux observation data. The relatively sparse observations in China introduce significant uncertainties in regional carbon sink estimations. While Long Short-Term Memory (LSTM) models have been widely applied to remote sensing image time-series analysis and vegetation index prediction, their use in carbon sink prediction remains limited. This study assesses the ability of the LSTM model to predict NEE dynamics in typical Chinese forest ecosystems using ChinaFLUX data and multi-source remote sensing data. Using longterm Eddy Covariance (EC) observation data from 11 forest sites, alongside meteorological information and multi-source remote sensing data, we analyzed the carbon sink characteristics of five typical forest types: Deciduous Broadleaf Forest (DBF), Deciduous Needleleaf Forest (DNF), Evergreen Needleleaf Forest (ENF), Evergreen Broadleaf Forest (EBF), and Mixed Forest (MF). The results indicate that the LSTM model effectively captures the main trends of NEE, though some fluctuations persist in predictions for certain data points. During training and testing, the average R² values between model-predicted NEE and EC-derived NEE were 0.83 and 0.73, respectively, with RMSE values ranging from 9.75 to 31.04 g C m⁻² mon⁻¹. Furthermore, this study identifies key driving factors behind NEE variations across forest types. Environmental factors and vegetation physiological conditions exhibit significantly differing impacts on NEE. This study offers theoretical foundations and technical support for improving forest carbon sink assessments in China and informing climate change responses. It also presents a novel approach for accurately predicting and evaluating forest carbon sink dynamics.

1. Introduction

Forests, as the primary carbon sinks of terrestrial ecosystems, cover approximately one-third of Earth's land surface and absorb a net 2–3 Pg C annually (Harris et al., 2021; Pan et al., 2011). Chinese forests, being the main carbon sinks in the East Asian monsoon region, play a critical role in maintaining the global carbon balance. However, current estimates of forest carbon sinks exhibit substantial uncertainties, significantly limiting accurate assessments for national carbon emission management and climate change mitigation strategies(Zhu et al., 2023). Thus, improving the accuracy of forest carbon sink predictions is essential for achieving national carbon inventories and mitigating climate change risks.

Net Ecosystem Exchange (NEE), defined as the net CO₂ flux between an ecosystem and the atmosphere per unit area and time, directly quantifies carbon balance(Chapin et al., 2006). Eddy Covariance (EC) is the standard method for measuring NEE and a cornerstone of micrometeorology(Baldocchi et al., 1996). The eddy covariance (EC) observation method possesses a solid physical foundation and requires minimal theoretical assumptions, enabling long-term, continuous, and non-destructive monitoring of water, heat, and carbon fluxes(Gong et al., 2020). Consequently, an increasing number of researchers are utilizing EC observations to investigate the dynamic changes of ecosystem carbon fluxes and their relationships with environmental factors(Sun et al., 2019). Running (Running et al., 1999)emphasized that integrating flux tower data, models, and remote sensing data can significantly

enhance the accuracy of carbon flux estimates. The China Terrestrial Ecosystem Flux Observation Research Network (ChinaFLUX) comprises EC-based flux observation towers distributed across forest ecosystems throughout China(Chu et al., 2021). In recent years, commemorating the 20th anniversary of ChinaFLUX, China has opened access to more site-scale flux observation data from terrestrial ecosystems(Yu et al., 2024). This newly released dataset includes 26 sites, 7 of which are forest sites (https://www.nesdc.org.cn/, data as of June 2025). These latest open-access ChinaFLUX data provide significant potential for improving the simulation accuracy of NEE across China's terrestrial ecosystems. However, due to limitations of the EC method, such as demanding topographic requirements and susceptibility to meteorological conditions, employing data science approaches to analyze historical NEE observation data and advance better NEE simulation methods represents a critical current research trend.

Currently, a significant volume of research and projects is employing diverse machine learning (ML) and deep learning (DL) methods to predict carbon fluxes in terrestrial ecosystems. Commonly used models include Random Forests(Guo et al., 2023), Artificial Neural Networks (ANNs)(Kang et al., 2019), Support Vector Machines (SVMs)(Xu et al., 2018), Convolutional Neural Networks (CNNs)(Qian et al., 2024), and Long Short-Term Memory networks (LSTMs)(Huang et al., 2024). Among these, Long Short-Term Memory networks (LSTMs), a type of Recurrent Neural Network (RNN) featuring specialized gating mechanisms, incorporate feedback connections between neurons. This architecture enables them to capture longer-term temporal

dependencies and historical information far more effectively than standard RNNs(Hochreiter and Schmidhuber, 1997). While LSTM applications have been predominantly explored in domains such as meteorological forecasting(Siami-Namini et al., 2018), Natural Language Processing (NLP)(Liu, 2024), and time-series analysis of remote sensing imagery(Reddy and Prasad, 2018), their reliability has also been demonstrated in predicting vegetation indices(Besnard et al., 2019; Nathaniel et al., 2023). Crucially, the interannual variability (IAV) of ecosystem carbon fluxes is strongly governed by the memory effects of climatic and environmental drivers—phenomena rarely adequately represented in conventional modeling approaches. The inherent design of LSTMs, specifically their ability to learn and retain information over extended sequences, makes them uniquely suited to incorporate these critical climate-driven legacy effects on the carbon cycle. This capability addresses a fundamental limitation of traditional statistical and process-based models, which often struggle to capture the complex, lagged responses of ecosystems to antecedent conditions. Consequently, LSTMs hold substantial promise for significantly improving the spatial and temporal accuracy of regional forest carbon sink estimates, offering a more robust data-driven framework for understanding carbon dynamics. By explicitly modeling the temporal persistence of environmental influences, LSTMs offer a powerful approach to overcome the limitations of traditional methods and hold considerable promise for enhancing the accuracy of regional forest carbon sink quantification(Reichstein et al., 2019).

However, related simulation studies on predicting forest carbon sinks are still relatively scarce. More importantly, studies focused on the simulation and prediction of forest carbon sinks still suffers from large uncertainties due to the complexity of forest ecosystems and the limited application of purely ChinaFLUX observations with difficulty in data accessibility. This study is aimed to test the ability of LSTM in predicting Chinese forest NEE dynamics using ChinaFLUX observations and multi-source remote sensing data.

2. Study Area and Data

2.1 Study Area

The study area encompasses China's forests (Figure 1), which exhibit extensive spatial distribution and significant regional heterogeneity. The total area of closed-canopy forests is approximately 9.91×10^5 km². By forest type, DBF occupies the largest area $(3.65\times10^5$ km²), followed by EBF $(3.10\times10^5$ km²) and MF $(2.44\times10^5$ km²). ENF covers 6.50×10^4 km², while DNF is the least distributed $(7.36\times10^3$ km²).

ENF predominantly occurs in high-altitude humid regions of western Sichuan, northwestern Yunnan, and southeastern Tibet. EBF is primarily distributed across subtropical to tropical monsoon zones, including southern Yunnan, southern Guangxi, Guangdong, Hainan, Taiwan, and low mountain areas of Fujian, Jiangxi, Guizhou, Hunan, and southeastern Tibet. These forests thrive in warm, humid climates with abundant rainfall, featuring complex stand structures and high species diversity. EBF exhibits the highest carbon storage and sink capacity among all forest types. DNF is restricted to high-latitude cold-temperate zones, notably in northern Heilongjiang (e.g., Mohe) and northeastern Inner Mongolia (Hulunbuir). DBF displays distinct zonal characteristics across temperate monsoon regions, forming extensive contiguous stands in Northeast China (northern Heilongjiang, Jilin, and Liaoning), supported by the Changbai Mountains and southern Greater/Lesser Khingan ranges. MF primarily occurs in transitional humid subtropical-temperate zones, concentrated in

Southwestern mountainous areas (Sichuan, Yunnan, Guizhou), Central China (Hunan, Hubei, Jiangxi, southern Anhui), Eastern hills (northern Fujian, Guangdong), and Southeastern Jilin and Heilongjiang. Collectively, these distributions reflect substantial spatial heterogeneity in China's forest types.

Given the marked differences in geographical distribution, climatic adaptation, and carbon sink functionality across forest types, NEE prediction and driver analysis stratified by plant functional types (PFTs) are essential. This approach enhances model specificity and scientific rigor.

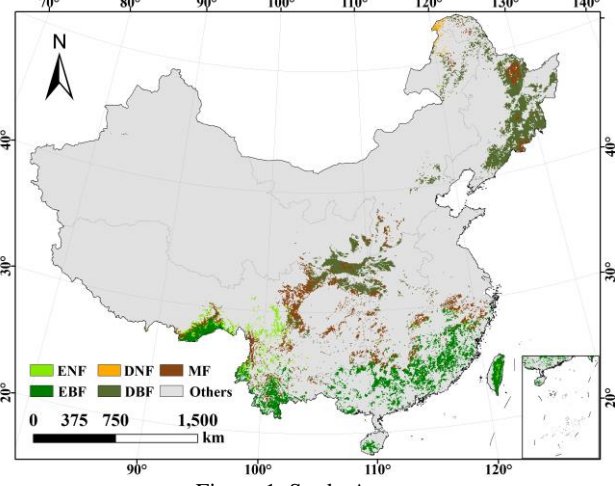


Figure 1. Study Area

2.2 Data Sources

This study utilized publicly available Net Ecosystem Exchange (NEE) data and selected 14 driving factors closely linked to NEE dynamics based on prior simulation research. These factors encompass both vegetation structural properties and environmental conditions.

To enhance simulation accuracy for Chinese forests, NEE data were specifically sourced from forest site flux observations publicly released by China's National Science & Technology Infrastructure (https://nesdc.org.cn/).

Drivers of NEE were categorized into two fundamental groups: (1) external environmental factors, including climate variables (e.g., temperature, precipitation, solar radiation)(Dusenge et al., 2019) and soil properties (e.g., soil moisture, soil temperature)(Lavergne et al., 2020); and (2) internal vegetation state factors involving structural and physiological characteristics such as Leaf Area Index (LAI), forest age, and NDVI(Niinemets, 2023). Crucially, vegetation growth processes—including photosynthesis and respiration—respond interactively to both environmental conditions and vegetation state dynamics.

3. Methodology

3.1 Fundamental Principles of the LSTM

Long Short-Term Memory (LSTM), a specialized Recurrent Neural Network (RNN) variant, overcomes the vanishing gradient problem inherent in standard RNNs when modeling long-term dependencies. While RNNs maintain sequential memory through inter-time-step information transfer, their inability to learn distant temporal relationships due to gradient attenuation is resolved by LSTM's persistent cell state and gated mechanisms. This architecture propagates information throughout sequences without

constant modification via three critical components: the forget gate determines obsolete information to discard, the input gate regulates new relevant data integration, and the output gate controls contextual information emission at each time step. Thereby, LSTMs selectively retain essential features across extended sequences, significantly outperforming standard RNNs in long-dependency applications—including speech recognition, language modeling, and time-series forecasting—through superior capture of complex temporal patterns(Kaadoud et al., 2022).

3.2 Input Configuration of the LSTM Model: Feature Variables and Hyperparameter Settings

This study investigates five typical forest ecosystems in China using long-term EC observations from 11 forest sites, complemented by meteorological parameters (e.g., temperature, precipitation) and multi-source remote sensing data (e.g., forest age, SIF, LAI, NDVI). The dataset comprises 8,820 individual measurements aggregated into 588 site-month records. We employed LSTM modeling to predict NEE for five major forest types: DBF, DNF, MF, EBF, and ENF. For LSTM implementation, key hyperparameters—including hidden layer dimensionality, learning rate, weight decay coefficient, epoch count, batch size, and dropout rate—were optimized through systematic grid search. Approximately 3,600 hyperparameter combinations were evaluated per forest type to identify optimal configurations prior to prediction. The LSTM model is as follows:

$$NEE_{t} = LSTM \begin{pmatrix} TEMP_{t-w:t} \\ PRE_{t-w:t} \\ VPD_{t-w:t} \\ WD_{t-w:t} \\ WS_{t-w:t} \\ P_{t-w:t} \\ PAR_{t-w:t} \\ FAPAR_{t-w:t} \\ VWC_{t-w:t} \\ TS_{t-w:t} \\ AGE_{t-w:t} \\ SIF_{t-w:t} \\ LAI_{t-w:t} \\ NDVL \\ NDVL \end{pmatrix}$$

$$(1)$$

where NEE_t represents the NEE value at time t, $LSTM(\cdot)$ indicates the LSTM model learning and predicting from the input multivariate time series data, and t-w denotes the time series input from the previous w time steps up to the current time t (time window), which is used to capture temporal dynamics. (TEMP, PRE, VPD, WD, WS, P, PAR, FAPAR, VWC, TS, AGE, SIF, LAI, and NDVI represent temperature, precipitation, vapor pressure deficit, wind direction, wind speed, atmospheric pressure, photosynthetically active radiation, fraction of photosynthetically active radiation, volumetric water content, soil temperature, forest age, solar-induced chlorophyll fluorescence, leaf area index, and normalized difference vegetation index, respectively).

3.3 Evaluation Metrics for Model Accuracy

We applied three metrics to evaluate the accuracy of the trained LSTM-NEE models, including the coefficient of determination (R²), mean absolute error (MAE), and root mean square error (RMSE). The definitions of these metrics are given as follows:

$$R^{2} = 1 - \frac{\sum_{i=1}^{n} (y_{i} - \hat{y}_{i})^{2}}{\sum_{i=1}^{n} (y_{i} - \bar{y})^{2}}$$
(2)

$$MAE = \frac{1}{n} \sum_{i=1}^{n} |y_i - \hat{y}_i|$$
 (3)

$$RMSE = \sqrt{\frac{1}{n} \sum_{i=1}^{n} (y_i - \hat{y}_i)^2}$$
 (4)

where y_i represents the true value, \hat{y}_i represents the predicted value, and $\bar{y} = \frac{1}{n} \sum_{i=1}^{n} y_i$ represents the mean of the true values, and n is the sample size.

3.4 SHAP-based Analysis of the Influencing Factors of NEE for Different Vegetation Types

SHAP (SHapley Additive exPlanations) is a unified framework for interpreting machine learning models by assigning feature importance values to individual predictions. Grounded in cooperative game theory's Shapley values, it establishes additive feature attribution models where predictions are represented as linear combinations of each feature's marginal contribution. The SHAP framework satisfies three fundamental axioms: Local accuracy, attribution values sum to the model's prediction; Missingness, features not present in the input receive zero attribution; Consistency, increased feature influence never decreases attribution value. These properties ensure theoretically consistent and practically feasible explanations for complex models.

In this study, SHAP analysis identifies key drivers of Net Ecosystem Exchange (NEE) across vegetation functional types. We implement regression modeling for regional NEE prediction coupled with SHAP to quantify attribution differences in climatic, edaphic, hydrological, and structural factors. Through comparative assessment of feature importance, this approach reveals mechanistic controls on NEE variability while enhancing model interpretability. The resulting quantitative evidence advances understanding of ecosystem carbon balance drivers, supporting improved ecological process modeling, carbon sink assessment, and climate response research. The formal SHAP formulation is as follows:

$$f(x) = \varphi_0 + \sum_{i=1}^{M} \varphi_i \tag{5}$$

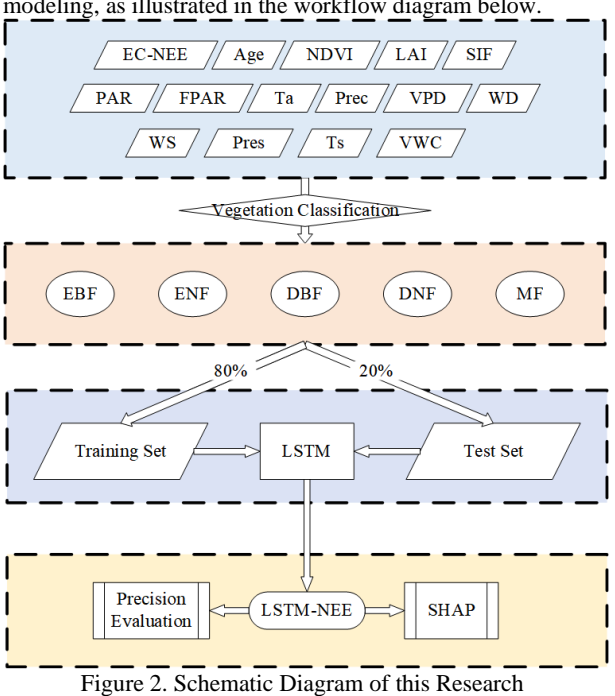
$$\varphi_{i} = \sum_{S \subseteq F \setminus \{i\}} \frac{|S|! \cdot (|F| - |S| - 1)!}{|F|!} [f(S \cup \{i\}) - f(S)] \quad (6)$$

$$\varphi_0 = E[f(z)] \tag{7}$$

where, f(x) denotes the predicted NEE value, φ_0 represents the baseline prediction (typically the mean output of training samples when all features are marginalized), φ_i represents the marginal contribution of the i-th feature to the model's prediction for the current sample, F denotes the complete feature set, and S denotes the subset of all features excluding the i-th feature. (Wang et al., 2024)

To summarize the methodology, this study commenced with

preprocessing raw data through screening, missing value imputation, and variable extraction, followed by stratifying samples into five vegetation functional types—EBF, ENF, DBF, DNF, and MF-with each dataset partitioned into training and testing subsets at an 80:20 ratio for LSTM modeling and prediction; during model training, Grid Search optimization identified optimal hyperparameter configurations (including architecture and learning parameters) per vegetation type, whereupon models trained with these configurations predicted NEE with performance validated via accuracy metrics (MSE, MAE, R2); to enhance interpretability, SHAP analysis was subsequently implemented for feature attribution, identifying dominant NEE drivers across vegetation types while quantifying their relative importance and revealing divergent ecological mechanisms-thus establishing theoretical foundations for ecosystem carbon budget regulation and providing methodological frameworks for climate-response ecological modeling, as illustrated in the workflow diagram below.



4. Results

4.1 Prediction Accuracy of NEE Across Different Forest Types Using the LSTM Model

The LSTM model estimated monthly NEE for flux sites across five Chinese forest types. Prediction accuracy varied among PFTs, as shown in Figure 3. DBF, DNF and MF achieved high accuracy, with strong agreement between model-predicted and EC-derived NEE in both training (R² = 0.87-0.91; RMSE = 9.75-31.04 g C m $^{-2}$ mon $^{-1}$) and testing phases (R² = 0.77-0.81; RMSE = 16.38-32.33 g C m $^{-2}$ mon $^{-1}$). Conversely, EBF and ENF demonstrated lower performance, particularly ENF in testing (R² = 0.61-0.63; RMSE = 11.73-22.81 g C m $^{-2}$ mon $^{-1}$). Collectively, mean R² values reached 0.83 (training) and 0.73 (testing), with RMSE ranging from 9.75 to 31.04 g C m $^{-2}$ mon $^{-1}$. These results indicate reliable predictive capability across forest types, though minor fluctuations persist in certain predictions.

4.2 Site-Level Evaluation of LSTM Predictive Performance Across Forest Types

To comprehensively evaluate the fitting capability of the LSTM

model for Net Ecosystem Exchange (NEE) time series variations across different forest ecosystems, this study selected five representative sites encompassing diverse Plant Functional Types (PFTs). It presents typical prediction results (Figure 4) illustrating scenarios such as optimal performance, strong modeling stability, favorable type-specific response, and instances of declining predictive performance. Among all sites, the JFF site (Mixed Forest, MF) demonstrated the best predictive performance. It achieved a test set coefficient of determination (R2) as high as 0.99 and a Root Mean Square Error (RMSE) of only 1.69 g C m⁻² mon⁻¹. This indicates that the LSTM model can capture the dynamic changes of NEE in this region with exceptional precision, with predicted values showing high consistency with observations in both amplitude and timing. These results highlight the model's maximum potential in areas with high-quality data and stable environmental signals. The CBF site (Mixed Forest, MF), covering a complete time series from 2003 to 2011, served as a crucial sample for evaluating the model's ability to capture longterm seasonal cycles. Predictions for this site were stable, with an R² of 0.92 and an RMSE of 13.79. The model successfully captured interannual fluctuations and seasonal peaks/valleys, validating the LSTM model's strong adaptability and robustness in modeling NEE seasonal dynamics within mid-to-high latitude mixed forests.

Among the different PFTs, the HZF site (Deciduous Needleleaf Forest, DNF), representing a typical deciduous forest, displayed good predictive performance (R²=0.91, RMSE=11.17). The model accurately reproduced the seasonal fluctuation patterns and peak timings of NEE, potentially attributable to the site's relatively distinct phenological cycles and clear seasonal driving mechanisms.

In contrast, predictive performance exhibited fluctuations at some sites, highlighting limitations in the model's adaptability to specific ecosystem types or time periods. At the BTF site (Deciduous Broadleaf Forest, DBF), while the test period R² was 0.89, the RMSE reached 19.48 g C m⁻² mon⁻¹ – significantly higher than the training period RMSE (9.17). This indicates a notable prediction bias in 2018, particularly during the summer carbon sink peak, where predictions showed clear underestimation. This reflects the model's insufficient responsiveness to extreme events or climatic anomalies.

Finally, the LDF (or QYF) site exhibited characteristics typical of limited model generalization capability. Taking LDF as an example, it performed well during the training period (R²=0.94), but its test period R² sharply dropped to 0.39 and the RMSE increased to 20.60, with predicted trends deviating from observations. Similarly, the QYF site (Evergreen Needleleaf Forest, ENF) consistently showed systematic underestimation throughout its time series (test R² only 0.30). This reflects the model's weaker capacity to capture the seasonal rhythm and underlying physiological mechanisms of carbon exchange in evergreen forest types. This limitation may be related to the lower intra-annual variability and more complex driving mechanisms characteristic of evergreen forests.

4.3 SHAP Analysis of NEE Drivers in Forest Ecosystems

SHAP analysis revealed significant interspecific divergence in dominant Net Ecosystem Exchange drivers across PFTs (Figure 5), reflecting distinct physiological adaptations to environmental forcing mechanisms. Deciduous forests exhibited pronounced SIF dominance, with contributions reaching 78.5% in DNF and 53.2% in DBF. This overwhelming influence establishes photosynthetic activity as the primary regulator of carbon dynamics in these

ecosystems. Conversely, evergreen forests demonstrated contrasting controls: VPD dominated ENF at 40.9% contribution, indicating water stress as a key constraint, while PAR governed EBF with 19.5% contribution supplemented by precipitation at 13.4%. Notably, LAI in ENF and VWC in EBF showed marginal effects of 1.7% and 1.4% respectively, demonstrating their limited regulatory roles. Mixed forest displayed a hybrid regulatory structure where air temperature functioned as the primary driver at 42.1% with SIF acting as significant secondary contributor at 19.9%. Wind speed and wind direction demonstrated minimal influence at 0.8% each. Crucially, both MF and EBF exhibited multiple key drivers, specifically TEMP and VPD in MF, and PAR and precipitation in EBF, demonstrating synergistic control of carbon exchange processes.

This study provides a new approach for simulating NEE in Chinese forests by integrating multi-source data, which contributes to a better understanding of the role of Chinese forest ecosystems in the terrestrial carbon cycle.

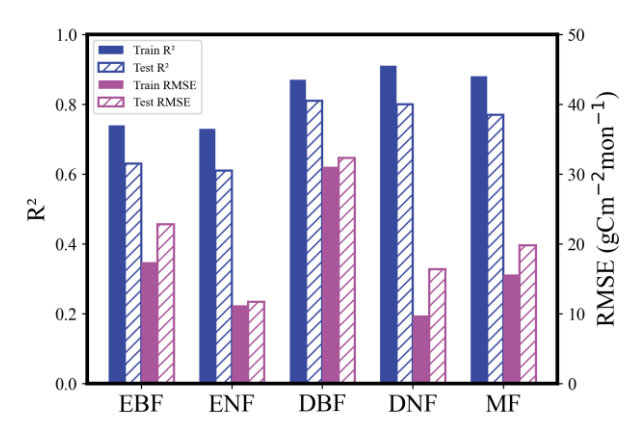


Figure 3. Model Performance Comparison Over Five Forest Types. (DBF: Deciduous Broadleaf Forest, DNF: Deciduous Needleleaf Forest, MF: Mixed Forest, EBF: Evergreen Broadleaf Forest, and ENF: Evergreen Needleleaf Forest). The units of RMSE are g C m⁻² mon⁻¹.

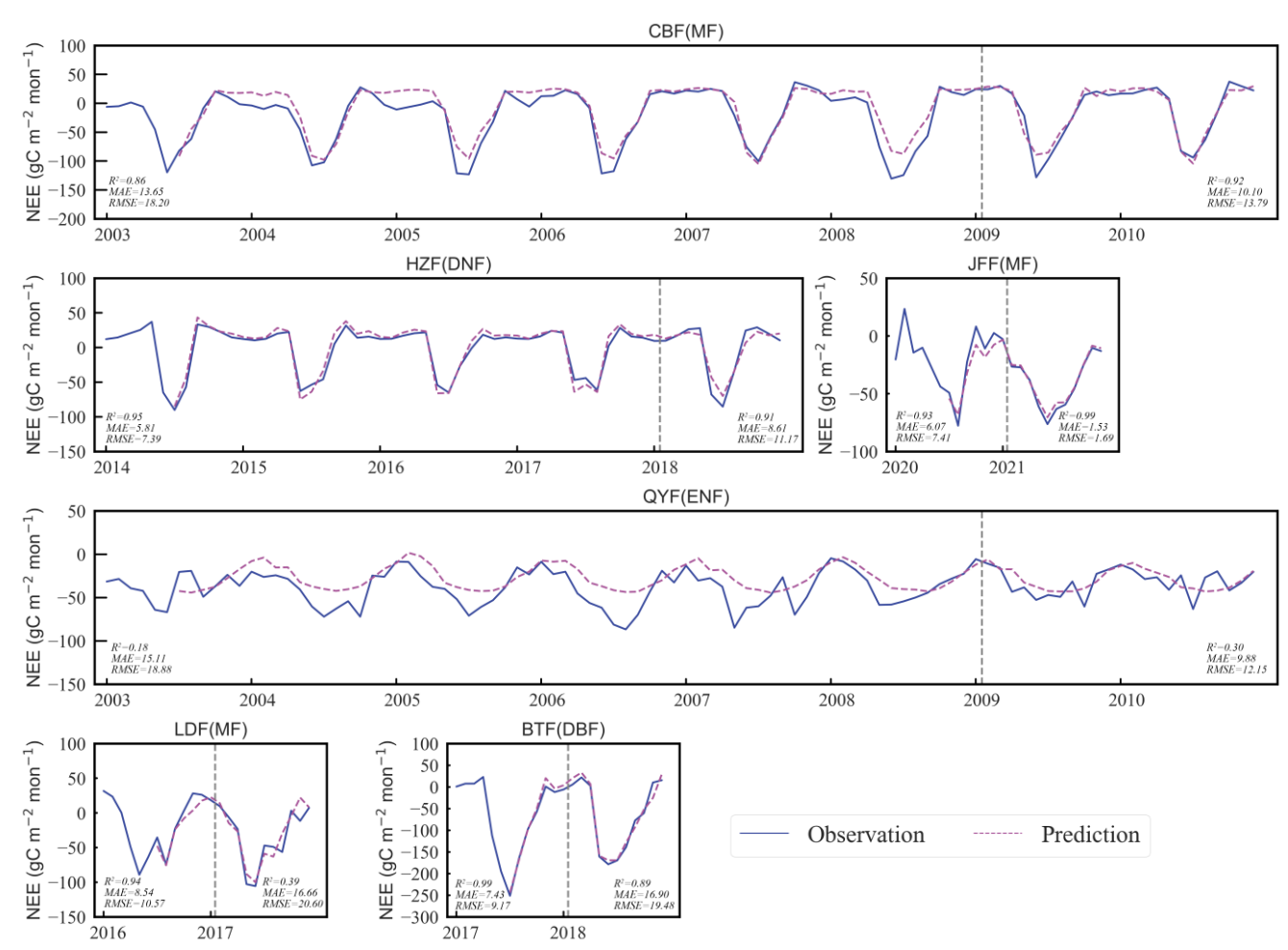


Figure 4. Comparison of Observed and Predicted NEE Across Representative Sites of different PFTs using LSTM and EC observations. (CBF: Changbai Mountain Station; HZF: Huzhong Station; JFF: Jinfoshan Station; QYF: Qianyanzhou Station; LDF: Xiaolangdi Station; BTF: Baotianman Station;). The gray dashed line indicates the start of the site testing period. It is important to note that in this study, the input data from the first six months were used to train the LSTM model, so there are no NEE predictions for the initial six months. The units for the RMSE and MAE are both grams of carbon per square meter per month (g C m⁻² mon⁻¹).

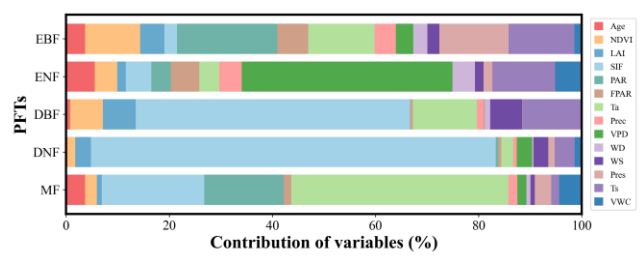


Figure 5. The relative contributions of forest age, normalized difference vegetation index, leaf area index, solar-induced chlorophyll fluorescence, photosynthetically active radiation, fraction of photosynthetically active radiation, temperature, precipitation, vapor pressure deficit, wind direction, wind speed, atmospheric pressure, soil temperature and volumetric water content to monthly NEE from the SHAP method across five Chinese typical forest ecosystems.

5. Conclusion

This study investigated carbon sink dynamics across five typical Chinese forest types by integrating long-term EC observations from 11 forest sites with meteorological parameters and multisource remote sensing data. The dataset comprised 8,820 individual measurements aggregated into 588 site-month records. LSTM modeling was employed to predict NEE for DBF, DNF, MF, EBF, and ENF.

Our results demonstrate robust predictive capability of LSTM across forest types, with stable performance despite minor fluctuations in isolated predictions. DBF, DNF, and MF exhibited high accuracy, achieving training $R^2 = 0.87 - 0.91$ and testing $R^2 = 0.77 - 0.81$, with RMSE ranging from 9.75 to 32.33 g C m^{-2} mon $^{-1}$. This confirms LSTM's effectiveness in simulating forest-type-specific NEE dynamics. However, EBF and ENF showed relatively lower precision, particularly ENF (testing $R^2 = 0.61$; RMSE = 11.73 - 22.81 g C m^{-2} mon $^{-1}$), indicating potential for model refinement in evergreen ecosystems.

SHAP-based driver analysis revealed significant vegetation-type-dependent controls on NEE , EBF: Dominated by photosynthetically active radiation (PAR; 19.47%) and precipitation (13.42%); ENF: Primarily regulated by vapor pressure deficit (VPD; 40.88%); Deciduous forests: SIF-driven (DBF: 53.21%; DNF: 78.52%), with negligible precipitation effects (0.05–0.52%); MF: Temperature-controlled (42.07%), supplemented by SIF (19.88%). These divergent driver hierarchies reflect fundamentally distinct carbon-regulation mechanisms across forest ecosystems.

While this work validates LSTM's site-level predictive capability and identifies PFT-specific drivers, future research will scale to China's entire forest domain. Incorporating additional ecological zones and remote sensing layers will enhance model generalizability, ultimately strengthening national carbon sink assessments and supporting evidence-based climate mitigation strategies.

Acknowledgements

This research was supported by the National Natural Science Foundation of China (Youth Fund) under Grant No.42201381 and the Program of Beijing Scholar.

References

Baldocchi, D., Valentini, R., Running, S., Oechel, W., and

Dahlman, R.: Strategies for measuring and modelling carbon dioxide and water vapour fluxes over terrestrial ecosystems, *Global change biology*, 2, 159-168, 1996.

Besnard, S., Carvalhais, N., Arain, M. A., Black, A., Brede, B., Buchmann, N., Chen, J., Clevers, J. G. W., Dutrieux, L. P., and Gans, F.: Memory effects of climate and vegetation affecting net ecosystem CO2 fluxes in global forests, *PloS one*, 14, e0211510, 2019.

Chapin, F. S., Woodwell, G. M., Randerson, J. T., Rastetter, E. B., Lovett, G. M., Baldocchi, D. D., Clark, D. A., Harmon, M. E., Schimel, D. S., and Valentini, R.: Reconciling carbon-cycle concepts, terminology, and methods, *Ecosystems*, 9, 1041-1050, 2006.

Chu, H., Luo, X., Ouyang, Z., Chan, W. S., Dengel, S., Biraud, S. C., Torn, M. S., Metzger, S., Kumar, J., and Arain, M. A.: Representativeness of Eddy-Covariance flux footprints for areas surrounding AmeriFlux sites, *Agricultural and Forest Meteorology*, 301, 108350, 2021.

Dusenge, M. E., Duarte, A. G., and Way, D. A.: Plant carbon metabolism and climate change: elevated CO 2 and temperature impacts on photosynthesis, photorespiration and respiration, *New Phytologist*, 221, 32-49, 2019.

Gong, Y., Ji, X.-f., Hua, Y.-t., Zhang, Y.-l., and Li, N.: Research progress of CO2 flux in forest ecosystem based on eddy covariance technique: a review, 2020.

Guo, R., Chen, T., Chen, X., Yuan, W., Liu, S., He, B., Li, L., Wang, S., Hu, T., and Yan, Q.: Estimating global GPP from the plant functional type perspective using a machine learning approach, *Journal of Geophysical Research: Biogeosciences*, 128, e2022JG007100, 2023.

Harris, N. L., Gibbs, D. A., Baccini, A., Birdsey, R. A., De Bruin, S., Farina, M., Fatoyinbo, L., Hansen, M. C., Herold, M., and Houghton, R. A.: Global maps of twenty-first century forest carbon fluxes, *Nature Climate Change*, 11, 234-240, 2021.

Hochreiter, S. and Schmidhuber, J.: Long short-term memory, *Neural computation*, 9, 1735-1780, 1997.

Huang, C., He, W., Liu, J., Nguyen, N. T., Yang, H., Lv, Y., Chen, H., and Zhao, M.: Exploring the potential of Long Short-Term Memory Networks for predicting net CO2 exchange across various ecosystems with multi-source data, *Journal of Geophysical Research: Atmospheres*, 129, e2023JD040418, 2024.

Kaadoud, I. C., Rougier, N. P., and Alexandre, F.: Knowledge extraction from the learning of sequences in a long short term memory (LSTM) architecture, *Knowledge-Based Systems*, 235, 107657, 2022.

Kang, M., Ichii, K., Kim, J., Indrawati, Y. M., Park, J., Moon, M., Lim, J.-H., and Chun, J.-H.: New gap-filling strategies for long-period flux data gaps using a data-driven approach, *Atmosphere*, 10, 568, 2019.

Lavergne, A., Sandoval, D., Hare, V. J., Graven, H., and Prentice, I. C.: Impacts of soil water stress on the acclimated stomatal limitation of photosynthesis: Insights from stable carbon isotope data, *Global Change Biology*, 26, 7158-7172, 2020.

- Liu, C.: Long short-term memory (LSTM)-based news classification model, *Plos one*, 19, e0301835, 2024.
- Nathaniel, J., Liu, J., and Gentine, P.: MetaFlux: Meta-learning global carbon fluxes from sparse spatiotemporal observations, *Scientific Data*, 10, 440, 2023.
- Niinemets, Ü.: Variation in leaf photosynthetic capacity within plant canopies: optimization, structural, and physiological constraints and inefficiencies, *Photosynthesis Research*, 158, 131-149, 2023.
- Pan, Y., Birdsey, R. A., Fang, J., Houghton, R., Kauppi, P. E., Kurz, W. A., Phillips, O. L., Shvidenko, A., Lewis, S. L., and Canadell, J. G.: A large and persistent carbon sink in the world's forests, *science*, 333, 988-993, 2011.
- Qian, L., Yu, X., Wu, L., Zhang, Z., Fan, S., Du, R., Liu, X., Yang, Q., Qiu, R., and Cui, Y.: Improving high uncertainty of evapotranspiration products under extreme climatic conditions based on deep learning and ERA5 reanalysis data, *Journal of Hydrology*, 641, 131755, 2024.
- Reddy, D. S. and Prasad, P. R. C.: Prediction of vegetation dynamics using NDVI time series data and LSTM, *Modeling Earth Systems and Environment*, 4, 409-419, 2018.
- Reichstein, M., Camps-Valls, G., Stevens, B., Jung, M., Denzler, J., Carvalhais, N., and Prabhat, F.: Deep learning and process understanding for data-driven Earth system science, *Nature*, 566, 195-204, 2019.
- Running, S. W., Baldocchi, D., Turner, D., Gower, S. T., Bakwin, P., and Hibbard, K.: A global terrestrial monitoring network integrating tower fluxes, flask sampling, ecosystem modeling and EOS satellite data, *Remote sensing of environment*, 70, 108-127, 1000
- Siami-Namini, S., Tavakoli, N., and Namin, A. S.: A comparison of ARIMA and LSTM in forecasting time series, 2018 17th IEEE international conference on machine learning and applications (ICMLA), Orlando, Florida, USA2018.
- Sun, S., Che, T., Li, H., Wang, T., Ma, C., Liu, B., Wu, Y., and Song, Z.: Water and carbon dioxide exchange of an alpine meadow ecosystem in the northeastern Tibetan Plateau is energy-limited, *Agricultural and Forest Meteorology*, 275, 283-295, 2019.
- Wang, H., Liang, Q., Hancock, J. T., and Khoshgoftaar, T. M.: Feature selection strategies: a comparative analysis of SHAP-value and importance-based methods, *Journal of Big Data*, 11, 44, 2024.
- Xu, T., Guo, Z., Liu, S., He, X., Meng, Y., Xu, Z., Xia, Y., Xiao, J., Zhang, Y., and Ma, Y.: Evaluating different machine learning methods for upscaling evapotranspiration from flux towers to the regional scale, *Journal of Geophysical Research: Atmospheres*, 123, 8674-8690, 2018.
- Yu, G.-R., Chen, Z., and Wang, Y.-P.: Carbon, water and energy fluxes of terrestrial ecosystems in China, 2024.
- Zhu, J. H., Tian, Y., Li, Q., Liu, H. Y., Guo, X. Y., Tian, H. L., Liu, C. F., and Xiao, W. F.: The current and potential carbon sink in forest ecosystem in China, *Acta Ecologica Sinica*, 43, 3442-3457, 10.5846/stxb202205201425, 2023.